



Prediction of fracture risk of a distal femur reconstructed with bone cement: QCSRA, FEA, and in-vitro cadaver tests

Hoda Mosleh¹ · Gholamreza Rouhi¹ · Azadeh Ghouchani¹ · Nima Bagheri²

Received: 29 October 2018 / Accepted: 27 January 2020 / Published online: 3 February 2020
© Australasian College of Physical Scientists and Engineers in Medicine 2020

Abstract

Lack of quantitative, biomechanical criteria to predict the risk of fracture for a bone affected by giant cell tumor (GCT) has made the decision for the necessary surgical technique a dilemma. The purpose of this study is to critically assess the usefulness of quantitative computed tomography (QCT) based structural rigidity analysis (QCSRA) and QCT-based finite element analysis (FEA) in predicting the fracture risk for long bones reconstructed with bone cement. QCSRA, QCT-based FEA, and in-vitro mechanical tests on five pairs of cadaveric distal femora were employed to quantitatively assess the compressive failure load of the human femur affected by GCT and reconstructed with bone cement. QCT was utilized to investigate the bone's structural rigidity properties as well as to generate heterogeneous finite element models using written material mapping codes. In order to validate the QCSRA and QCT-based FEA results, their outcomes were compared with the results of in-vitro mechanical tests on human cadavers. Results of this study demonstrated an acceptable correlation between QCSRA fracture loads and fracture loads found in in-vitro mechanical tests on cadavers ($R^2=0.85$). Also, QCSRA procedure is developed in order to estimate the axial stiffness and the maximum bending stiffness of the bone, employing the QCT-scans. It is shown that these two features, describing the structural rigidity, are linked to the experimental fracture loads ($R^2=0.72$ for axial stiffness, $R^2=0.79$ for maximum bending stiffness). Moreover, a good correlation was found between the fracture loads determined by QCT-based FEA and the experimental in-vitro fracture loads ($R^2=0.92$). Results of this study confirm the usefulness of the applications of QCSRA and QCT-based FEA as clinically tools for predicting the failure load of a long bone.

Keywords Bone fracture · Quantitative computed tomography · Structural rigidity analysis · In-vitro mechanical tests · Finite element analysis · Failure load · Cadaveric femur

Introduction

Giant cell tumor (GCT) of bone is a benign, but aggressive lesion which has the potential for malignancy [1–3]. This tumor is prevalent in young people (20–40 years old), and GCT mostly affects the metaphyseal–epiphyseal area of long bones and the bones participating in the knee joints, i.e. the distal femur and proximal tibia are the first and second persistent sites of this kind of tumor [2, 4, 5]. Treatment of a bone affected by GCT is a truly challenging issue [6] because there is no clinical, radiological or histological

dimension that allows the physician to predict the tumor progression or metastases [3]. Various methods including surgery, radiotherapy, and chemotherapy are used for the treatment of GCT [5]. A surgical process is still the most common treatment for GCT and usually includes tumor removal with the curettage technique and then defect reconstruction, which may be challenging for the surgeon as there are many different approaches [7]. Reconstruction is performed by filling the cavity with bone cement or graft, and in some cases where the size of the cavity is large the use of internal stabilizers including screws, plates, or nails is essential to reduce the risk of fracture [5, 8, 9]. One important concern regarding the surgical process is that in most cases the technique of tumor removal and reconstruction is based solely on the surgeons' experience [10, 11], and a fundamental problem after the reconstruction is postoperative bone fracture [12]. The fracture risk of the bone can be quantified by evaluation of the size and location of the

✉ Gholamreza Rouhi
grouhi@aut.ac.ir

¹ Faculty of Biomedical Engineering, Amirkabir University of Technology, Tehran, Iran

² Tehran University of Medical Science, Tehran, Iran

tumor and through analysis of a patient's bone mineral density (BMD) [13]. True assessment of the bone mineral density in the body can improve the prediction and detection of fracture risk as well as its treatment. Quantitative computed tomography (QCT) is the unique modality that measures the real bone density in a determinate volume (mg/cm^3) without the overlapping of others tissues, and differently from dual-energy x-ray absorptiometry (DXA), it allows a selective assessment of both trabecular and cortical bone [14]. Some of the advantages of QCT, compared to other imaging techniques, are as follows: volume density can be obtained, trabecular and cortical BMDs can also be separately determined, and its high sensibility for assessing trabecular BMD [14]. Structural rigidity is a property that integrates both the material and geometric properties of bone. Alteration in the structural rigidity of a bone, induced by the disease and afflicted with defects, can represent changes occurring in the tissue's material and geometric properties [15]. Quantitative computed tomography based structural rigidity analysis (QCSRA) can be used to monitor changes in bone geometry and material properties by assessing axial, bending, and torsional rigidities [16]. These characteristics provide a fine biomechanical model of bone geometry and material properties [17]. QCT is more accurate and efficient than the DXA method, which does not differentiate between cancellous and dense bone, and other common radiographic procedures, such as an MRI, for predicting the risk of bone fractures [14]. QCT can be preferable to DXA-aBMD in clinical studies for predicting femoral strength [18]. In addition, QCSRA has shown greater sensitivity, 100% versus 66.7%, and specificity, 60.6% versus 47.9%, than Mirels' scoring criterion for predicting pathologic fracture in femoral bone lesions [19].

Finite element analysis (FEA) and modelling have gained considerable attention in biomechanical research and can have wide applications. FE modelling can simulate different experimental conditions and develops much more data analysis than what can be done in a laboratory; thus, it decreases the time and expenses of in vivo and in-vitro experimentations. Accurate FE models of bone, using QCT images, can predict the fracture risk of a bone with a simulated defect similar to what is seen following GCT surgery [5]. Accordingly, FE models can be a valuable tool to improve clinical fracture risk predictions in metastatic bone disease [20]. To date, there are few studies in which computer simulation approaches for GCT surgeries were utilized [12].

The main scope of this work was to evaluate the usefulness of QCSRA and QCT-based FEA through statistical-based comparisons of data determined by the two different procedures on the fracture risk of a bone reconstructed with bone cement. In order to validate the QCSRA and QCT-based FEA results, their outcomes were compared with the results of in-vitro mechanical tests on human cadavers.

Materials and methods

This study consists of both computational and experimental parts. The computational section is divided into two parts: QCSRA, and QCT-based FEA. In the QCSRA section, the failure load was calculated for the weakest cross-section of a long bone; in the QCT-based FEA section, the failure load was calculated when the displacement was applied to a distal femur model. In the experimental section, the cadaveric bone samples were loaded under uniaxial compression and the failure load was recorded for each sample. Finally, the results of the experimental section were used to check the validity of the results determined by the computational section.

Specimen preparation

In this study, ten (five pairs) cadaveric distal femoral bones (4 males and 1 female, aged from 39 to 64) were provided by the Central Bank of Organ Transplantation, University of Tehran, and all soft tissue around each sample was carefully removed by an orthopedic surgeon. Based on previous studies, the critical defect volumes at high risk of fracture were considered for the ratio of tumor to distal femur volume of 40% to 60% [21, 22]. Therefore, in this study, the ratios of tumor volume to distal femur volume were considered to be: 30%, i.e. less than their critical values; 50%, i.e. an average of critical value; and 70%, i.e. more than their critical values (Table 1). Moreover, the tumor was simulated in: the medial and lateral; the epiphysis-metaphysis; and the epiphysis (alone) regions. Table 1 provides detailed information about the cadaveric specimens, location, and size of cavities made by an orthopedic surgeon.

In each pair of specimens, part of the bone of the left femur was removed by an orthopedic surgeon, and the cavity was carefully made and then filled with radiopaque and

Table 1 Specifications of cadaveric samples, their age, size, and location of cavity

Sample #	Specification of sample	Size (volume removed/distal femur volume) and anatomical location of cavity
1	64-Year-old male	30%, medial, epiphysis-metaphysis
2	58-Year-old male	50%, medial, epiphysis-metaphysis
3	39-Year-old male	70%, medial, epiphysis-metaphysis
4	34-Year-old male	50%, medial, epiphysis
5	46-Year-old female	50%, lateral, epiphysis-metaphysis

self-curing acrylic bone cement (Sulcem™³ Gentamicin, Sulzer Medica, Switzerland) (Fig. 1(1)). The right femur of the same individual was left intact and considered as the control sample.

QCT image processing

The defective femur samples were placed inside a container filled with water and QCT scans were carried out using a clinical scanner (Siemens-Somatom 64, 140 kV, 80 mAs, 0.5 × 0.5 mm/pixel resolution, and 1 mm slice thickness). Consecutive images were also taken from the bone cross-section by the QCT. A calibration phantom (Mindways Software, Inc., San Francisco, CA) with five tubes and specified reference material densities were used to convert the Hounsfield units (HUs) to bone mineral density. Figure 1(2) presents a view of the scanner, imaging, as well as a section of a sample embedded in the imaging phantom.

Mechanical tests on cadaveric bones

Bone samples were mechanically tested by a dynamic testing machine (Hct400/25, Zwick/Roellin, Germany). The specimens were loaded with a pre-load of 50 N at a quasi-static rate of 1 mm/min in uniaxial compression until they failed [23–25]. An indenter made of steel with a diameter of 20 mm and a flat surface was applied to the medial condyle of the samples, which were fixed in a cylinder with a diameter of 70 mm (Fig. 1(3)). The length of the specimens was between 170 and 240 mm, and the mean size of the embedded specimens was 40 mm. A load–displacement curve was recorded for each specimen. The maximum load in each curve was considered as the bone’s failure strength [24].

Structural rigidity analysis

Structural rigidity analysis was utilized to predict the failure load based on the weakest cross-sectional area of a long bone. In this method, a Matlab code written to convert the Hounsfield units (HUs) obtained from QCT images to bone mineral density (ρ) was used to determine the modulus of elasticity (E) of each voxel using the relationships that exist between bone mineral density (ρ , g.cm⁻³) and its modulus of elasticity (E , MPa) (Table 2) [26].

ImageJ software (version 1.50i) was used to identify the maximum and minimum principal axes for each cross section of the images taken from QCT-scans of the bone that were obtained with 1 mm slice spacing. Then, using another code written in Matlab, incorporating the relationships in Table 2 and the equations below (Eqs. 1–4), the axial (EA) and bending (EI) rigidities at each trans-axial cross section was calculated. The neutral axes’ positions (\bar{x} , \bar{y}), EA, and EI were found, using Eqs. 1, 2, 3 and 4, respectively:

$$\bar{x} = \frac{\sum_{i=1}^n x_i E_i \Delta a}{\sum_{i=1}^n E_i \Delta a}, \bar{y} = \frac{\sum_{i=1}^n y_i E_i \Delta a}{\sum_{i=1}^n E_i \Delta a} \tag{1}$$

Table 2 Relation between bone density and its modulus of elasticity [26]

E– ρ relationship	Density range
$E = 33,900 \rho^{2.20}$	$\rho \leq 0.27$
$E = 5307 \rho + 469$	$0.27 < \rho < 0.6$
$E = 10,200 \rho^{2.01}$	$\rho \geq 0.6$

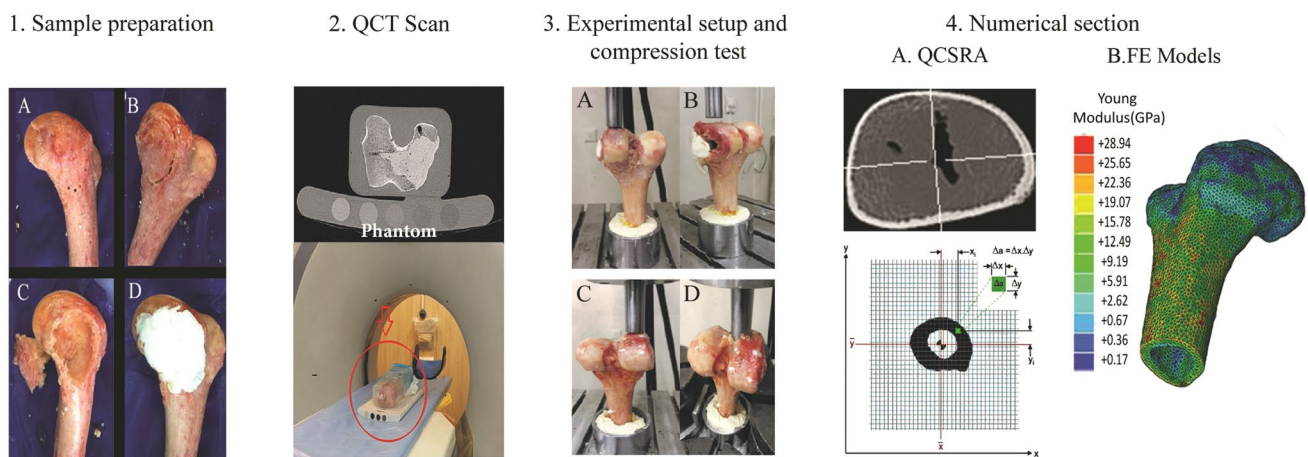


Fig. 1 Preparation of cadaveric human bone samples (femur) with defects, filled with bone cement: A drilling bone samples, B connecting holes, C creating cavity, and D filling the cavity with bone cement; 2 QCT scanning and the calibration phantom; 3 Mechanical

testing of ‘defected’ bone samples: A before failure (left femur), B after failure (left femur); and ‘intact’ bone samples: C before failure (right femur), D after failure (right femur); and 4 Numerical analyses: A QCSRA and B FE Models, Young’s modulus distribution

$$EA = \sum E_i(\rho)\Delta a \quad (2)$$

$$EI_y = \sum [E_i(\rho).x_i^2]\Delta a \quad (3)$$

$$EI_x = \sum [E_i(\rho).y_i^2]\Delta a \quad (4)$$

where ρ is the bone density, x_i and y_i are the distances of each pixel from the y and x axes, respectively, Δa represents each pixel's area, E_i shows Young's modulus of elasticity of the i th pixel. Modulus weighted neutral axis and centroid, Eq. (1), were calculated based on the coordinates of the i th pixel, its modulus (E_i), area (Δa), and total number of pixels at the bone cross-sectional (n). Axial rigidity, Eq. (2), was calculated by summing the products of elastic modulus of each pixel (E_i) and its area (Δa). Bending rigidity about y-axis, Eq. (3), is the sum of the products of the elastic modulus (E_i), square of the distance of the i th pixel to the neutral axis (x_i^2), and the pixel area (Δa), and bending rigidity about x-axis, Eq. (4), is the sum of the products of the elastic modulus (E_i), square of the distance of i th pixel to the neutral axis (y_i^2), and the pixel area (Δa) (Fig. 2) [16].

The cross section with the lowest structural rigidity, i.e. the lowest axial stiffness (EA) and the lowest bending stiffness (EI_{MAX}), were considered as the weakest cross sections [15, 16, 27]. Finally, the fracture load, F_{QCSRA} , based on the QCSRA, axial, and bending rigidities of the weakest cross

section were determined using the MATLAB code. In order to define F_{QCSRA} , the structural stiffness parameters was merged with simple beam theory, as follows [16]:

$$F_{QCSRA} = \frac{\epsilon_{Critical} \times EA \times EI_{MAX}}{(EI_{MAX} + (EA \times y \times d))} \quad (5)$$

where $\epsilon_{Critical}$ is the critical strain at bone failure, E is the average elastic modulus of the weakest cross section ($N.mm^{-2}$), A is the cross sectional area (mm^2); I_{MAX} is the maximum moment of inertia (mm^4) at the weakest cross section, y is the distance to the bone surface from geometric centroid, where critical stress occurs, and d is the distance from the applied load to the geometric centroid at the weakest cross sectional area. In defining a QCSRA based failure load (F_{QCSRA}), the critical strain which identifies the onset of fracture ($\epsilon_{Critical}$) was assumed to be 1.2% strain in compression, and 1% strain in tension [16, 28–30].

Finite element analysis

In the FEA, the failure load should be determined in order to be able to predict fracture risk [16]. For this purpose, Mimics Software v10.01 was first employed to create a solid 3D model of a femur with bone cement inserted in it using QCT images. Then, the 3D model was imported to ABAQUS CAE 6.14, by considering an isotropic, linear elastic, but heterogeneous model of the bone; and an isotropic, linear elastic and homogenous model for the bone cement insert (Fig. 1(4)B). In the FEA material mapping codes, based on QCT images, were written in Python to automatically assign heterogeneous material properties to each element of the bone and bone cement. A Poisson's ratio of 0.3 was assumed for the bone model [16]. The interface between the femur and cement was assumed to be tied [12]. Although hexahedral are known to be more accurate than tetrahedral elements [25, 31], Due to the complexity of the geometry, quadratic ten node tetrahedral elements type was used in this study. The maximum stress, which occurred in the condylar region in all models, was used for evaluating the mesh quality. It was assumed that a suitable mesh density was obtained when the increase in the stress was less than 5% in two different element sizes. The mesh density was selected based on a mesh sensitivity analysis; hence the number of elements and element size in each model were approximately between 171,000–222,000 and between 0.8–2.3 mm, respectively. In this work, a static analysis was performed in the computational models and to mimic in-vitro tests conditions, the end of femur's diaphysis were assumed to be fully fixed and represented the boundary conditions in the FE models, and An axial compressive displacement was applied on some nodes on the medial condyle of the bone, which were located

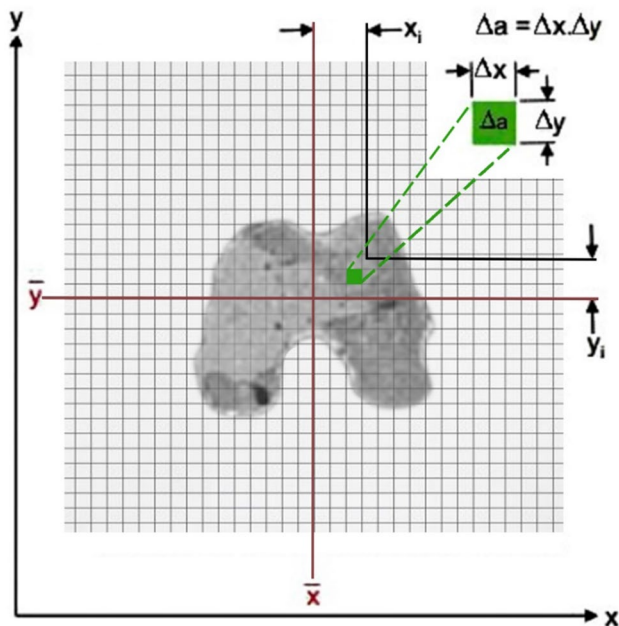


Fig. 2 Schematic diagram illustrating the pixel-based QCSRA technique to calculate axial (EA) and bending (EI) rigidities. Each grid element is intended to represent one pixel

on a circular shape region with the diameter equals to the indenter diameter, used in the experiment.

Statistical analysis

Linear regression analysis was used to compare the fracture loads calculated by FEA, as well as by QCSRA, with the mechanical tests' results. In this work, statistical differences between the resulting regression lines and the slope and interception of the $y = x$ line were calculated. Linear regression was also performed for fracture loads resulting from the mechanical tests on cadaveric bones and structural stiffness parameters including EA and EI_{Max} . The correlation coefficient (R^2) was used as a criterion to compare each of the methods with the experimental test. Statistical analysis was performed using SPSS software V.21, and P values less than 0.05 ($P < 0.05$) were considered statistically significant.

Results

The mechanical tests failure loads for the defective and control femurs are shown in Table 3. Others results of this study are shown in Fig. 3.

Outcomes from this study demonstrated an acceptable correlation between QCSRA fracture loads and fracture loads found in the in-vitro cadaveric tests ($R^2 = 0.85$) (Fig. 3A). Moreover, the results of regression analysis showed that the slope of the regression curve did not deviate from the $y = x$ line [$F_{Mech} = 0.8734F_{QCSRA} + 0.9558$] ($P = 0.72$). In addition, the y-intercept was also shown to be not significantly different from zero ($P = 0.30$) (Fig. 3A). Good agreement was also observed between axial stiffness (EA), maximum bending stiffness (EI_{Max}), and the experimental fracture loads ($R^2 = 0.72$, $R^2 = 0.79$, respectively) (Fig. 3B, C). The finite element analysis, as stated above, was performed to find the fracture loads based on a linear elastic, isotropic, but heterogeneous model of bone; it showed a good correlation with the experimental fracture loads on cadaveric bones ($R^2 = 0.92$) (Fig. 3D). Figure 3D indicates that the slope of the relationship between FEA

failure loads and cadaveric test results is very close to 1 [$F_{Mech} = 1.0805F_{FEA} + 0.109$] ($P = 0.34$), and the y-intercept was also shown to be not significantly different from zero ($P = 0.87$).

Results of the QCSRA analysis method presented here also confirmed that bone generally fails at a strain of 1.2% in compression, which is independent of its Young modulus of elasticity. Previous studies have also indicated that the fracture strain of bone is independent of its modulus of elasticity [16, 28–30]. The correlations in Fig. 3 indicate that the proposed methods, QCSRA and QCT-based FEA, were considered appropriate approaches for the prediction of fracture risk in a long bone affected, for instance, by giant cell tumor and reconstructed with bone cement.

Discussion and conclusions

In-vitro mechanical tests on human cadavers and FEA are crucial and helpful tools in determining an appropriate surgical method within the scope of minimizing the risk of postoperative fracture [5, 20, 25, 31]. This research was conducted to achieve a quantitative understanding of the failure load in a distal femur affected by GCT and reconstructed with bone cement by utilizing the QCT based FEA, QCT based structural stiffness technique, and in-vitro mechanical tests on human cadavers to study uniaxial compressive load. The compressive axial load was applied to mimic the normal physical activity of standing [32]. In this study, control samples were used to assess the reduced failure load in defective femurs as compared to healthy femurs. Moreover, results of the defective bones simulated by FEA and QCSRA were compared with the data collected from mechanical test made on defective cadaveric samples.

Results of the experimental tests on each pair of healthy and defective bone showed that due to reduced structural bone properties, the maximum load of distal femora reconstructed with the bone cement varied between 60 and 90% of the maximum load of a healthy bone, depending on the cavity size (see Table 3). As Figs. 3B, C show, good correlations were resulted between structural rigidities, i.e. EA and EI_{Max} , and experimental failure loads of cadavers ($R^2 = 0.72$ and $R^2 = 0.79$ for EA and EI_{Max} , respectively). This implies that calculation of structural rigidities, even without calculating the critical load by QCSRA (Eq. 5), can provide an acceptable prediction of the fracture load, and thus it can be employed as a convenient tool in predicting the fracture risk of a long bone.

One of the novel aspects of this study was the use of material mapping codes in the finite element simulation to take into account bone heterogeneity, as opposed to the previous studies in which bone was assumed to be a homogeneous structure [25, 31, 33, 34]. Using material mapping codes,

Table 3 Values of failure loads determined by mechanical tests for the defected and control femurs

Sample	Failure load (N) (defected samples) mechanical tests	Failure load (N) (control samples) mechanical tests
64-Year-old male	2543	4253
58-Year-old male	4568	6441
39-Year-old male	4751	6104
34-Year-old male	5008.8	5625.6
46-Year-old female	3315	4697

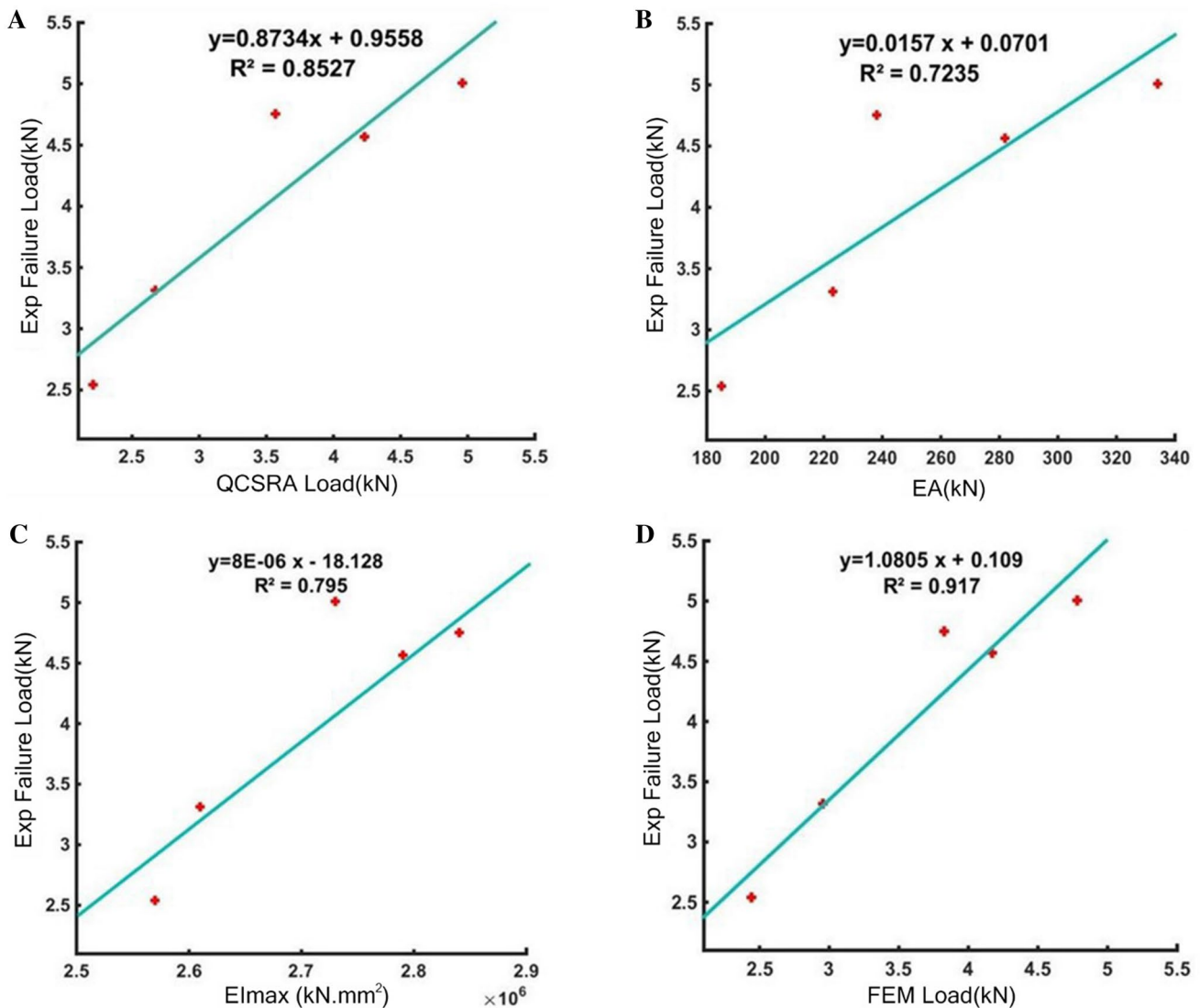


Fig. 3 Linear regression of: **A** experimental failure loads on cadavers vs. QCSRA loads; **B** experimental failure loads on cadavers vs. EA of the weakest cross section; **C** experimental failure loads on cadav-

ers vs. EI_{Max} of the weakest cross section; and **D** experimental failure loads on cadavers vs. FEA loads

density and Young's modulus were assigned to each element in the finite element model based on their density. The advantage of using material mapping codes, based on QCT images, is an automatic allocation of heterogeneous material properties to the bone. Thus, due to the fact that bone is a heterogeneous material, employing QCT based images in the in silico models can provide a more accurate prediction of bone mechanical behavior. Results of previous research have shown that non-homogenous material distribution is an important factor in determining the mechanical behavior of biological tissues [34], and other studies have indicated that the correlation coefficient in a non-homogenous model was better than a homogenous model ($R^2 = 0.79$ – 0.88 , $R^2 = 0.32$ – 0.48 , respectively) [15, 35]. Results of this work

show that relatively high correlation coefficients between QCSRA and mechanical testing data were evident in fracture loads ($R^2 = 0.72$, 0.79 and 0.85 , between EA, EI and QCSRA approaches, respectively, and cadaveric mechanical tests data). Results of this work are also in a good agreement with some previous clinical studies [16, 27]. The correlation coefficient between the results of the FEA, nonhomogeneous model, and in-vitro experimental failure loads obtained in mechanical tests on cadaveric samples, i.e. $R^2 = 0.92$, were similar to those obtained in other FEA studies [16, 24, 27, 36, 37]. The results of this study, despite some simplifications made in this work such as considering linear elastic properties and isotropic behavior for bone, imply that structural stiffnesses and finite element procedures are promising

approaches for assessing bone fracture risk ($R^2=0.85$ for QCSRA and $R^2=0.92$ for FEA compared to those of in-vitro mechanical tests data on cadavers).

Analysis of structural stiffness with simple beam theory can provide the fracture load for any bone cross-section based on QCT images. FEA presents stress and strain distribution and can also provide a detailed assessment of fracture loads. The main advantage of QCSRA and FEA, which are based on fundamental principles of engineering mechanics, is their noninvasive nature, and that they can be used to reliably identify patients at high risk of fracture [15]. Another important advantage of the proposed methods for predicting bone fracture load is their patient-specific application enabling the inclusion of each specific bone geometry as well as its precise density and Young's moduli distribution, which can provide a very good estimation of that specific bone strength and thus its fracture risk [16, 17].

One of the limitations of this work was to disregard muscles' forces in the FE model as well as in the QCSRA method. Due to the diverse range of patients' activities, the actual loads applied to the bones are unknown, therefore it is not possible to apply the actual clinical loads in FEA and QCSRA. Another limitation of the method presented in this research was that it exposes the patients to relatively high doses of radiation for getting QCT-scan images [15]. Despite the high accuracy of the finite element method, the time needed to calculate the fracture load using FEA for each sample was more than 10 h, employing an Apple Macbook Air 2015 with a Core i5 (15-5250U) CPU. This is remarkably greater than the time needed for calculating the stiffness related parameters and the fracture load using structural stiffness analysis, i.e. less than 30 min on the same computer. Nonetheless, it should be emphasized that finite element simulation is more appropriate than QCSRA for the implementation of complex loading conditions. Thus, based on the results of this work, it seems reasonable to suggest that one can use either QCSRA or FEA to provide an acceptable estimation of the bone fracture load under different conditions, and one may not need to make expensive and time consuming in-vitro tests on cadavers in order to collect a large experimental data set.

Another limitations of this study was the small number of cadavers. The FEA models made in this study were limited to isotropic material properties and linear elastic material properties. Although theoretically it would be possible to incorporate anisotropic properties of bone into the models, it is not possible to derive subject-specific anisotropic mechanical properties from clinical QCT scans [38, 39]. Considering the main scope of this study, which was to evaluate the usefulness of the two methods, QCSRA and FEA, for fast and accurate prediction of the failure load of the distal femur reconstructed with bone cement in clinical setting, our results show that linear FE analysis is shown to

be much faster than that of a nonlinear model with a similar prediction of fracture loads. A previous study comparing the computational time and accuracy of linear and nonlinear FE models demonstrated a significantly greater time, i.e., 96 times greater for non-linear models than that of the linear model with a similar accuracy between the two models [24].

Another novel aspect of this work was the simultaneous applications of QCSRA and QCT-based heterogeneous FEA as well as in-vitro cadaveric tests to predict the risk of fracture in a long bones affected by GCT and reconstructed with the bone cement. Thus, despite some simplifications made in this work such as considering linear elastic properties and isotropic behavior for bone, results of this work indicate that QCSRA and QCT-based FEA methods were used to gain a good estimation of the fracture risk in a long bone affected by the GCT and reconstructed with bone cement. Current criteria for identifying patients at high risk of post-operative fracture are not comprehensive, this is partly due to ignoring or underestimating the impact of patient-specific factors, i.e., bone geometry and its density distribution. Results of this study show the effectiveness and usefulness of the two computational methods, QCSRA and FEA, by considering patient-specific factors in predicting the strength of a bone reconstructed with bone cement as the key determinant of a bone fracture risk. The goal of this research was to present a non-invasive, fast, and reliable method that can be used to predict a long bone fracture load in patients affected by GCT before surgical intervention by an orthopedic surgeon. The presented method can be extended to investigate the effect of defect size and location on the bone fracture load, hence reinforcing the in-use criteria.

Acknowledgements The authors would like to thank Physio-Mechanical Characterization of Biomaterial Lab at Amirkabir University of Technology; Iranian Tissue Bank and Research Center of Tehran University of Medical Sciences, as well as Dr. S.H. Akhlaghpour for his support with the QCT scanning at Noor Medical Imaging Center, Tehran.

Funding There is no funding source.

Compliance with ethical standards

Conflict of interest The authors declare that they have no conflict of interest.

Ethical approval This article does not contain any studies with human participants or animals performed by any of the authors.

References

1. Cowan RW, Singh G (2013) Giant cell tumor of bone: a basic science perspective. *Bone* 52(1):238–246

2. Anwar Ul Haque AM (2008) Giant cell tumor of bone: a neoplasm or a reactive condition? *Int J Clin Exp Pathol* 1(6):489
3. Singh S, Singh M, Mak I, Ghert M (2013) Expressional analysis of GFP-tagged cells in an in vivo mouse model of giant cell tumor of bone. *Open Orthop J* 7:109–113
4. Balke M, Neumann A, Szuhai K, Agelopoulos K, August C, Goshager G, Hogendoorn PC, Athanasou N, Buerger H, Hagedorn M (2011) A short-term in vivo model for giant cell tumor of bone. *BMC Cancer* 11(1):241
5. Ghouchani A, Rouhi G (2017) The great need of a biomechanical-based approach for surgical methods of giant cell tumor: a critical review. *J Med Biol Eng* 37(4):454–467
6. Chakarun CJ, Forrester DM, Gottsegen CJ, Patel DB, White EA, Matcuk GR Jr. (2013) Giant cell tumor of bone: review, mimics, and new developments in treatment. *RadioGraphics* 33(1):197–211. <https://doi.org/10.1148/rq.331125089>
7. Ayerza MA, Aponte-Tinco LA, Farfalli GL, Lores Restrepo CA, Muscolo DL (2009) Joint preservation after extensive curettage of knee giant cell tumors. *Clin Orthop Relat Res* 467(11):2845–2851
8. Ruskin J, Caravaggi P, Beebe KS, Corgan S, Chen L, Yoon RS, Patterson FR, Hwang JS (2016) Steinmann pin augmentation versus locking plate constructs. *J Orthop Traumatol* 17(3):249–254
9. Bickels J, Meller I, Malawer M (2004) The biology and role of cryosurgery in the treatment of bone tumors. *Musculoskeletal cancer surgery*. Springer, Dordrecht, pp 135–145
10. Benevenia J, Rivero SM, Moore J, Ippolito JA, Siegeman DA, Beebe KS, Patterson FR (2017) Supplemental bone grafting in giant cell tumor of the extremity reduces nononcologic complications. *Clin Orthop Relat Res* 475(3):776–783
11. Chanasakulniyom M, Aroonjarattham K, Aroonjarattham P, Saktaveekulkit N, Sitthiseripratip K, Mahaisavariya B (2011) The effect of distal femur after replace with biomaterials: finite element analysis. In: The second TSME international conference on mechanical engineering Krabi, pp 19–21
12. Li J, Wodajo F, Theiss M, Kew M, Jarmas A (2013) Computer simulation techniques in giant cell tumor curettage and defect reconstruction. *Comput Sci Eng* 15(2):21–26
13. Rennick JA (2012) Bone fracture prediction using computed tomography based rigidity analysis and the finite element method. Northeastern University
14. D'Elia G, Caracchini G, Cavalli L, Innocenti P (2009) Bone fragility and imaging techniques. *Clin Cases Min Bone Metab* 6(3):234–246
15. Villa-Camacho JC, Iyoha-Bello O, Behrouzi S, Snyder BD, Nazarian A (2014) Computed tomography-based rigidity analysis: a review of the approach in preclinical and clinical studies. *BoneKEY reports* 3
16. Rennick JA, Nazarian A, Entezari V, Kimbaris J, Tseng A, Masoudi A, Nayeb-Hashemi H, Vaziri A, Snyder BD (2013) Finite element analysis and computed tomography based structural rigidity analysis of rat tibia with simulated lytic defects. *J Biomech* 46(15):2701–2709
17. Zhang M, Gao J, Huang X, Gong H, Zhang M, Liu B (2017) Effects of scan resolutions and element sizes on bovine vertebral mechanical parameters from quantitative computed tomography-based finite element analysis. *J Healthc Eng*. <https://doi.org/10.1155/2017/5707568>
18. Viceconti M, Qasim M, Bhattacharya P, Li X (2018) Are CT-based finite element model predictions of femoral bone strengthening clinically useful? *Curr Osteoporos Rep* 16(3):216–223
19. Damron TA, Nazarian A, Entezari V, Brown C, Grant W, Calderon N, Zurakowski D, Terek RM, Anderson ME, Cheng EY (2016) CT-based structural rigidity analysis is more accurate than mires scoring for fracture prediction in metastatic femoral lesions. *Clin Orthop Relat Res* 474(3):643–651
20. Eggermont F, Derikx L, Verdonschot N, Van der Geest I, De Jong M, Snyers A, Van der Linden Y, Tanck E (2018) Can patient-specific finite element models better predict fractures in metastatic bone disease than experienced clinicians? Towards computational modelling in daily clinical practice. *Bone Joint Res* 7(6):430–439
21. Jeys L, Suneja R, Chami G, Grimer R, Carter S, Tillman R (2006) Impending fractures in giant cell tumours of the distal femur: incidence and outcome. *Int Orthop* 30(2):135–138
22. Hirn M, de Silva U, Sidharthan S, Grimer RJ, Abudu A, Tillman RM, Carter SR (2009) Bone defects following curettage do not necessarily need augmentation: a retrospective study of 146 patients. *Acta Orthop* 80(1):4–8
23. An YH, Draughn RA (1999) Mechanical testing of bone and the bone-implant interface. CRC Press, Boca Raton
24. Mirzaei M, Keshavarzian M, Naeni V (2014) Analysis of strength and failure pattern of human proximal femur using quantitative computed tomography (QCT)-based finite element method. *Bone* 64:108–114
25. Samsami S, Saberi S, Sadighi S, Rouhi G (2015) Comparison of three fixation methods for femoral neck fracture in young adults: experimental and numerical investigations. *J Med Biol Eng* 35(5):566–579
26. Keyak JH, Falkinstein Y (2003) Comparison of in situ and in vitro CT scan-based finite element model predictions of proximal femoral fracture load. *Med Eng Phys* 25(9):781–787
27. Anez-Bustillos L, Derikx LC, Verdonschot N, Calderon N, Zurakowski D, Snyder BD, Nazarian A, Tanck E (2014) Finite element analysis and CT-based structural rigidity analysis to assess failure load in bones with simulated lytic defects. *Bone* 58:160–167
28. Hong J, Cabe GD, Tedrow JR, Hipp JA, Snyder BD (2004) Failure of trabecular bone with simulated lytic defects can be predicted non-invasively by structural analysis. *J Orthop Res* 22(3):479–486
29. Keaveny TM, Wachtel EF, Ford CM, Hayes WC (1994) Differences between the tensile and compressive strengths of bovine tibial trabecular bone depend on modulus. *J Biomech* 27(9):1137–1146
30. Snyder BD, Cordio MA, Nazarian A, Kwak SD, Chang DJ, Entezari V, Zurakowski D, Parker LM (2009) Noninvasive prediction of fracture risk in patients with metastatic cancer to the spine. *Clin Cancer Res* 15(24):7676–7683
31. Samsami S, Saberi S, Bagheri N, Rouhi G (2016) Interfragmentary motion assessment for three different fixation techniques of femoral neck fractures in young adults. *Bio-Med Mater Eng* 27(4):389–404
32. Ghouchani A, Rouhi G, Ebrahimzadeh MH (2019) Investigation on distal femoral strength and reconstruction failure following curettage and cementation: in-vitro tests with finite element analyses. *Comput Biol Med* 112:103360
33. Aroonjarattham P, Aroonjarattham K, Chanasakulniyom M (2015) Biomechanical effect of filled biomaterials on distal Thai femur by finite element analysis. *Kasetsart J Nat Sci* 49(2):263–276
34. Chang C-H, Hsu J-T, Chen S-I, Chen W-P, Chang G-L (2002) The effect of material inhomogeneous for femoral finite element analysis. *J Med Biol Eng* 22(3):121–128
35. Dall'Ara E, Pahr D, Varga P, Kainberger F, Zysset P (2012) QCT-based finite element models predict human vertebral strength in vitro significantly better than simulated DEXA. *Osteoporos Int* 23(2):563–572
36. Zysset PK, Dall'Ara E, Varga P, Pahr DH (2013) Finite element analysis for prediction of bone strength. *BoneKEY reports* 2
37. Wako Y, Nakamura J, Matsuura Y, Suzuki T, Hagiwara S, Miura M, Kawarai Y, Sugano M, Nawata K, Yoshino K (2018) Finite element analysis of the femoral diaphysis of fresh-frozen cadavers with computed tomography and mechanical testing. *J Orthop Surg Res* 13(1):192

38. Keyak JH, Kaneko TS, Tehranzadeh J, Skinner HB (2005) Predicting proximal femoral strength using structural engineering models. *Clin Orthop Relat Res* 437:219–228
39. Panyasantisuk J, Dall'Ara E, Pretterklieber M, Pahr D, Zysset P (2018) Mapping anisotropy improves QCT-based finite element estimation of hip strength in pooled stance and side-fall load configurations. *Med Eng Phys* 59:36–42

Publisher's Note Springer Nature remains neutral with regard to jurisdictional claims in published maps and institutional affiliations.